

Briefing Space Weather - 2022/04/18

Sun

Responsible: José Cecatto

CMEs to the Earth – SB arrival time

Date		
Apr, 11	6 CME can have a component toward the Earth;	Apr. 04 - 14 CME can have a component toward the Earth;
Apr, 12	4 CME can have a component toward the Earth;	Apr. 05 - 3 CME can have a component toward the Earth;
Apr, 13	6 CME can have a component toward the Earth *;	Apr. 06 - 4 CME can have a component toward the Earth;
Apr, 14	3 CME can have a component toward the Earth;	Apr. 07 - 4 CME can have a component toward the Earth;
Apr, 15	8 CME can have a component toward the Earth;	Apr. 08 - 3 CME can have a component toward the Earth;
Apr, 16	3 CME can have a component toward the Earth *;	Apr. 09 - 6 CME can have a component toward the Earth;
Apr, 17	6 CME can have a component toward the Earth *;	Apr. 10 - 3 CME can have a component toward the Earth;
Apr, 18	1 CME can have a component toward the Earth;	* Partial halo CME

Date
Apr, 11 – At 06:00 a halo CME
Apr, 12 - SB arrival time at 10:33 (CME occurred on April 09 at 12:00)
Apr, 13 – At 12:48 a partial halo CME; Arrival time at ~ 01:55 ?
Apr, 14 – SB arrival time at 03:37 (CME occurred on April 11 at 06:00), ass to geomagnetic storm; Arrival time ~ 12:35 ?
Apr, 15
Apr, 16 – At 10:12 a partial halo CME
Apr, 17 – At 03:48 a halo CME
Apr, 18

Summary

04/11 – Fast (< 550 km/s) wind stream; 6 CME can have component toward the Earth;

04/12 – Fast (< 550 km/s) wind stream; 4 CME can have component toward the Earth;

04/13 – Fast (< 500 km/s) wind stream; 6 CME can have component toward the Earth – 1 partial halo;

04/14 – Fast (< 600 km/s) wind stream; 3 CME can have component toward the Earth;

04/15 – Fast (< 600 km/s) wind stream; 8 CME can have component toward the Earth;

04/16 – Fast (< 650 km/s) wind stream; 3 CME can have component toward the Earth – 1 partial halo;

04/17 – Fast (< 550 km/s) wind stream; 6 CME can have component toward the Earth – 2 partial halo;

04/18 – Fast (< 600 km/s) wind stream; 1 CME can have component toward the Earth;

Prev.: Fast wind stream expected up to April 19; for while high (75% M, 25% X) probability of M / X flares next 2 days; also, occasionally other CME can present component toward the Earth.

Responsible: Douglas Silva

WSA-ENLIL (CME 2022-04-09T09:12Z)

- The simulation results indicate that the flank of CME will reach the DSCOVR mission between 2022-04-12T15:00Z and 2022-04-13T05:00Z.

WSA-ENLIL (CME 2022-04-11T06:00Z)

- The simulation results indicate that the flank of CME will reach the DSCOVR mission between 02:56Z and 16:56Z on April 14, 2022.

Coronal holes (SPOCA):

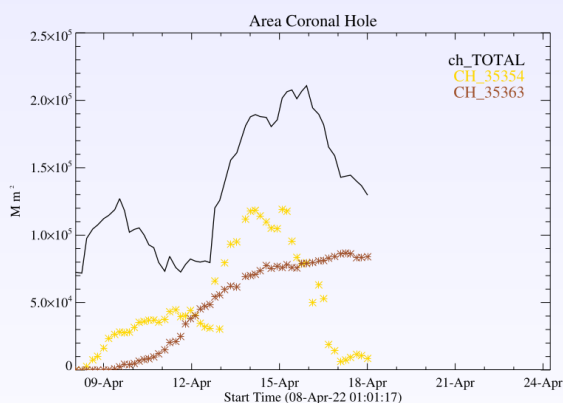


Figura: The solid line in black shows the products of the sum of areas for each detection interval performed by SPOCA between April 8th and 18th, 2022.

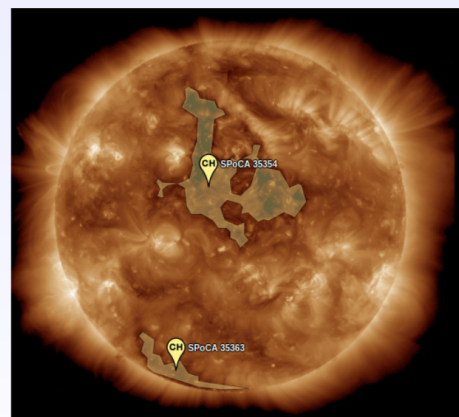
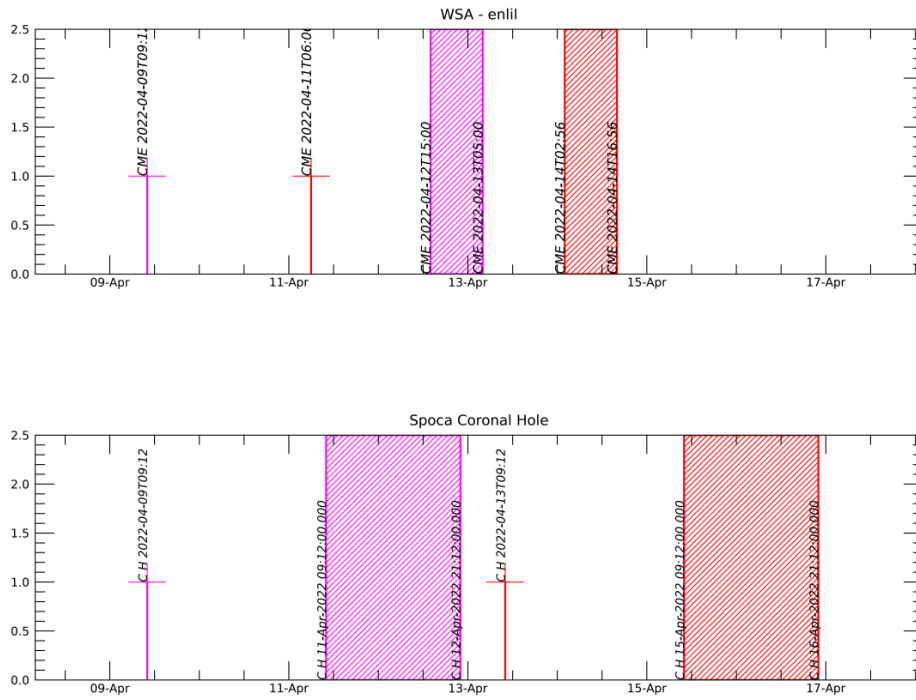


Figura: Above the 193 Å image of the Sun are highlighted coronal holes observed by SPOCA around 18:00 UT on April 13, 2022.

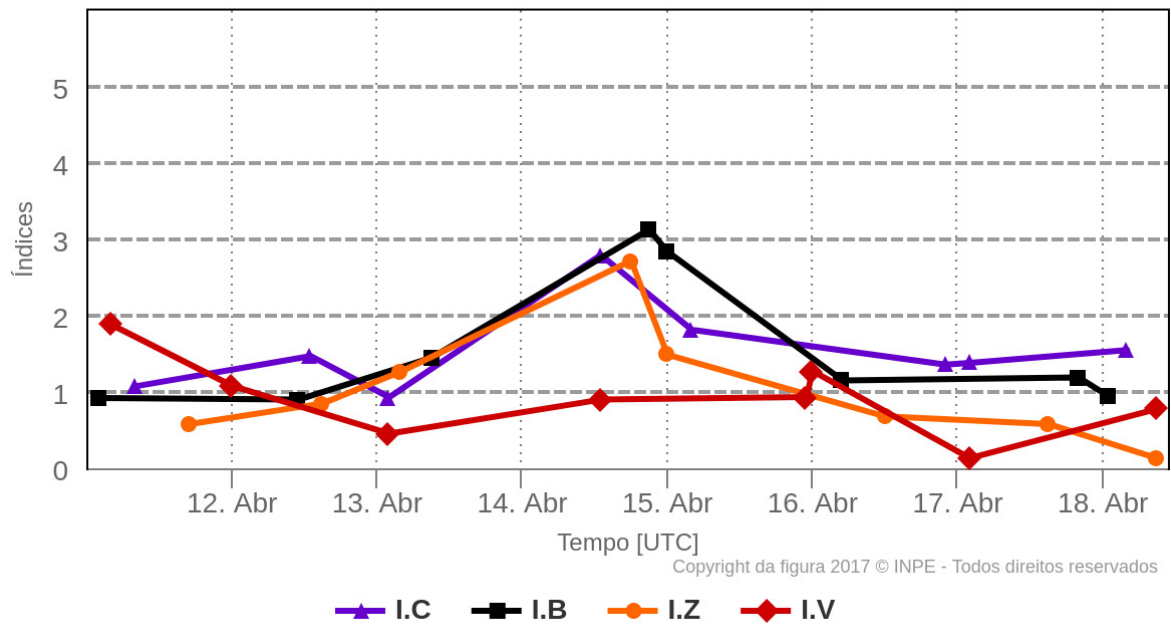
WSA - ENLIL SPOCA

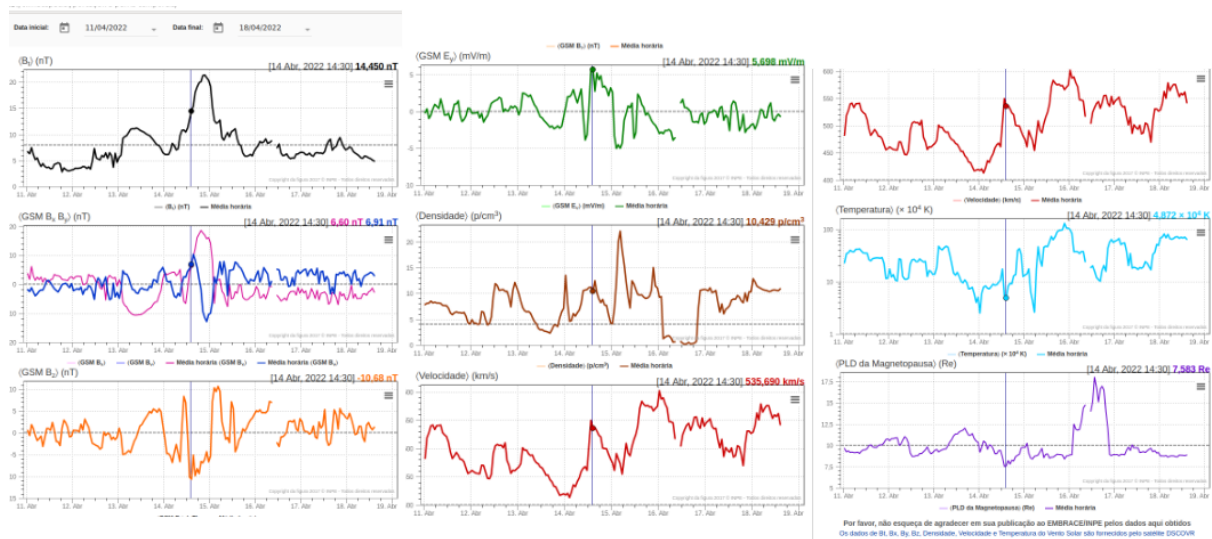
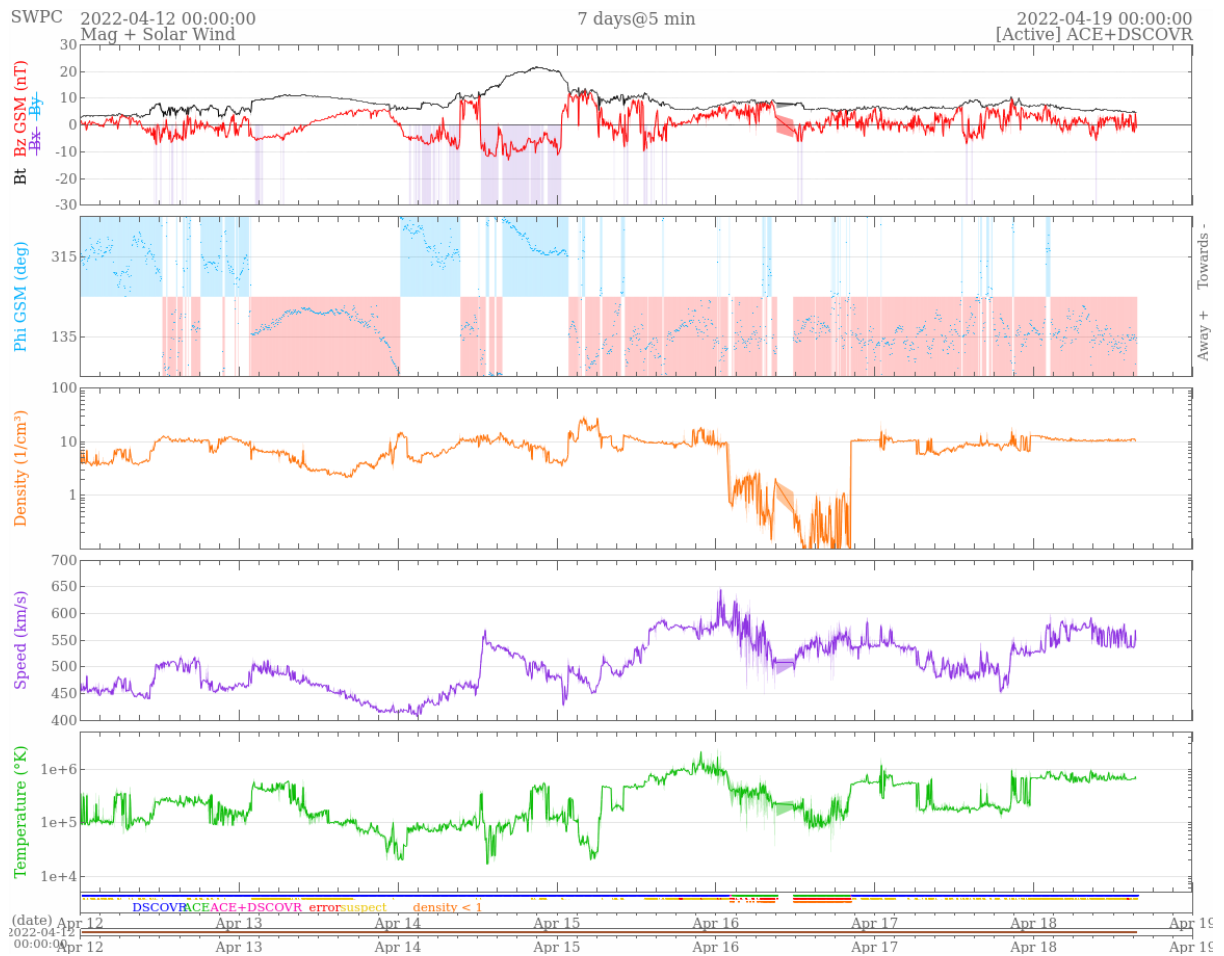


Responsible: Paulo Ricardo Jauer

Resumo dos índices do meio interplanetário

Máximos diários - mais recentes entre 11 Abr, 2022 e 18 Abr, 2022





- The modulus of the interplanetary magnetic field component showed 1 maximum peak: 14/Apr at 21:30 from ~ 21 nT.
- The BxB_y components showed intense variations in the analyzed period, due to the magnetic cloud characteristic with rotation initiated in the components on Apr/13 at 01:30 UT.

- The component of the bz field presented a rotation due to the magnetic cloud-like interplanetary structure. The minimum value presented in the bz component was -10.68 nT on Apr/14 at 14:30 UT. Conditions favorable to the emergence of geomagnetic storms
- The solar wind density showed a maximum peak on April 15th at 04:30 UT of 22.05 p/cm³. However, the density presented variations before and after this maximum peak due to the interaction of the fast solar wind and CME.
- The solar wind speed had oscillated mostly above 400 km/s throughout the presenting period. It presented a minimum value on 014/Apr at 02:30 of 412km/s, it also presented a maximum value of 601 km/s at 00:30 on 16/Apr.
- The position of the magnetopause was oscillating on average below the typical position. The maximum compression was observed on 14/Apr at 14:30 UT at 7.58 Re.

Radiation Belts

Responsible: Ligia Alves Da Silva

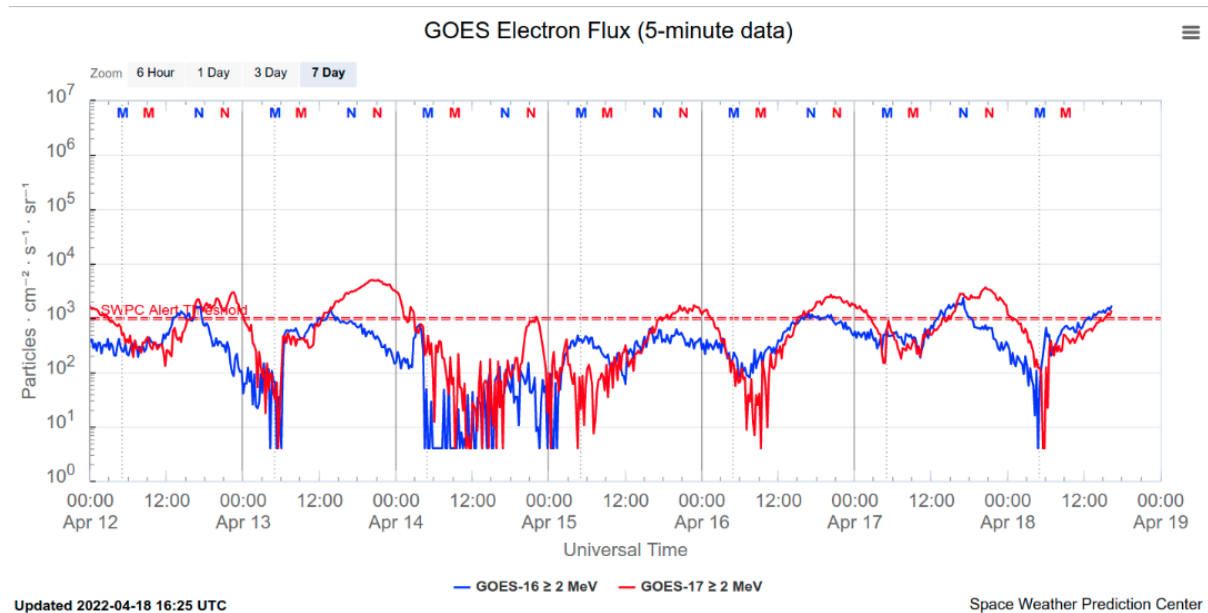


Figure 1: High-energy electron flux (> 2MeV) obtained from GOES-16 and GOES-17 satellite.

Source:

<https://www.swpc.noaa.gov/products/goes-electron-flux>

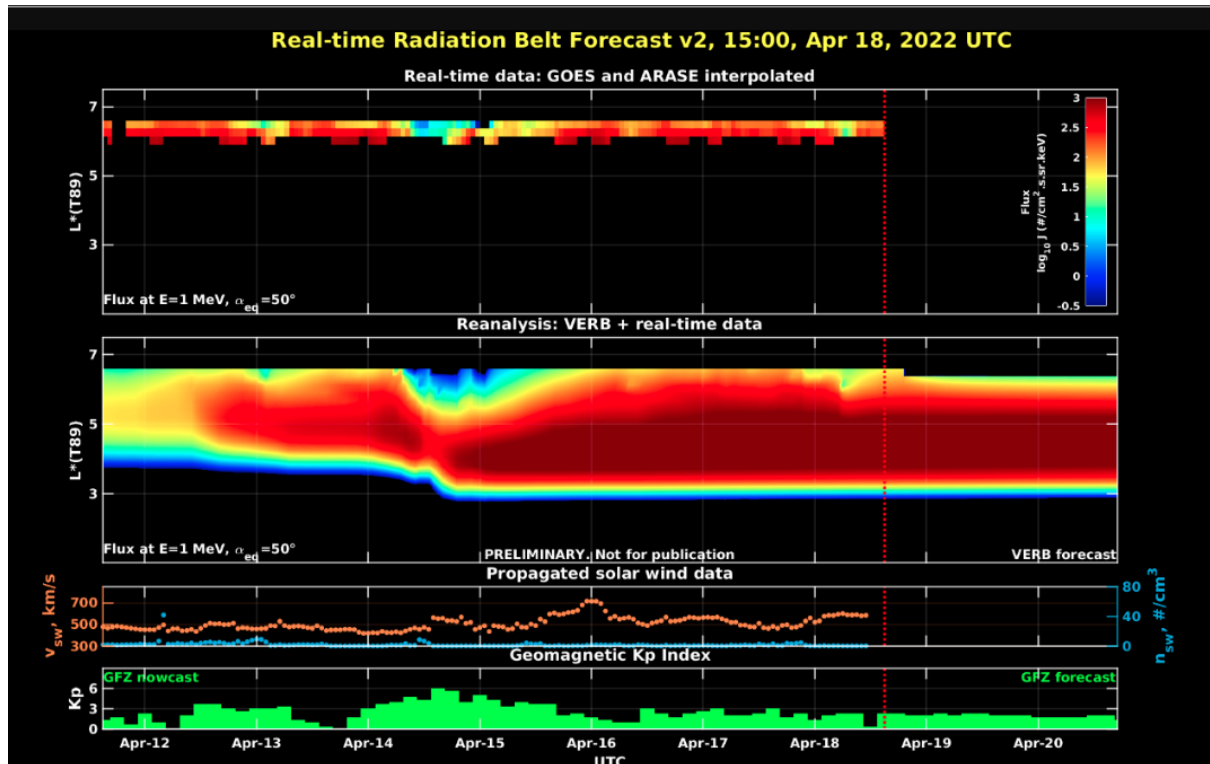


Figure 2: high-energy electron flux data (real-time and interpolated) obtained from ARASE, GOES-16, GOES-17

satellites. Reanalysis's data from VERB code and interpolated electron flux. Solar wind velocity and proton density data from ACE satellite. Source: <https://rbm.epss.ucla.edu/realtime-forecast/>

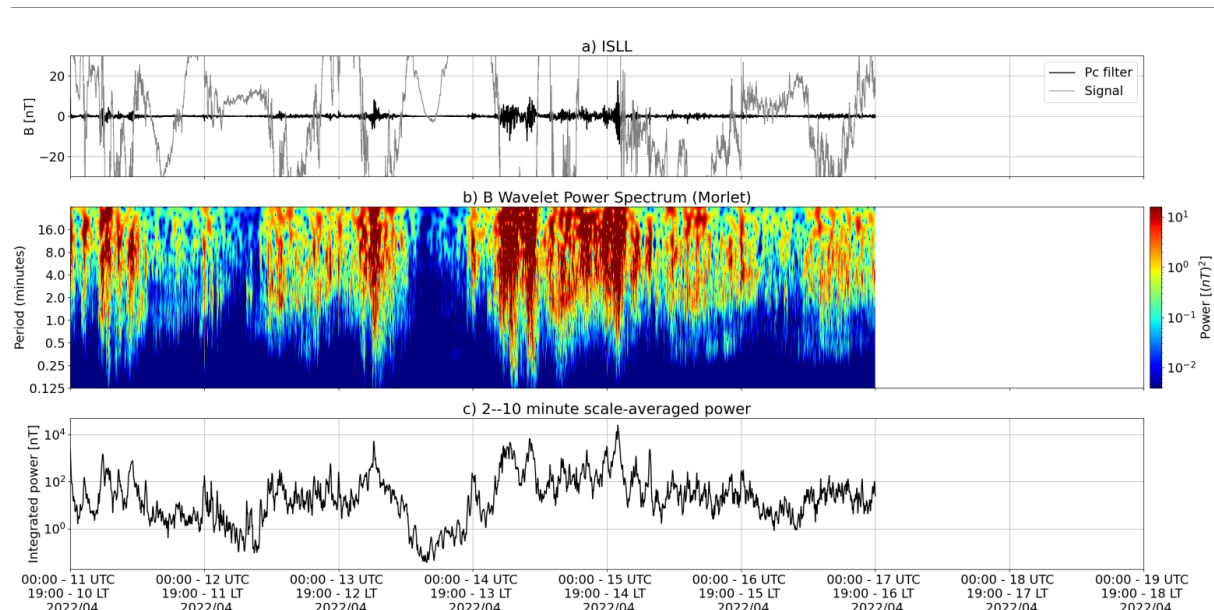
High-energy electron flux (>2 MeV) in the outer boundary of the outer radiation belt obtained from geostationary satellite data GOES-16 and GOES-17 (Figure 1) is oscillating around the minimum threshold (103 particles/(cm² s sr)) on April 12th. An electron flux decrease of approximately 2 orders of magnitude is observed on April 13th, while an electron flux decrease of approximately 3 orders of magnitude persists until mid-April 15. A rapid and slight electron flux decrease was observed on 18/April.

The GOES-16, GOES-17, and Arase satellite data are analyzed and interpolated to observe the high-energy electron flux variability (1 MeV) in the outer radiation belt (Figure 2). Additionally, the VERB code rebuilds this electron considering the Ultra Low Frequency (ULF) waves' radial diffusion. The simulation (VERB code) shows that the electron flux decreases observed on April 14th and 15th reached L-shell > 5.0, while the others reached only the boundary of the outer radiation belt. These variations in electron flux occurred concomitantly with the arrival of complex solar wind structures (coronal mass ejections and high-speed streams) and ULF wave activities. However, it is important to point out that the data

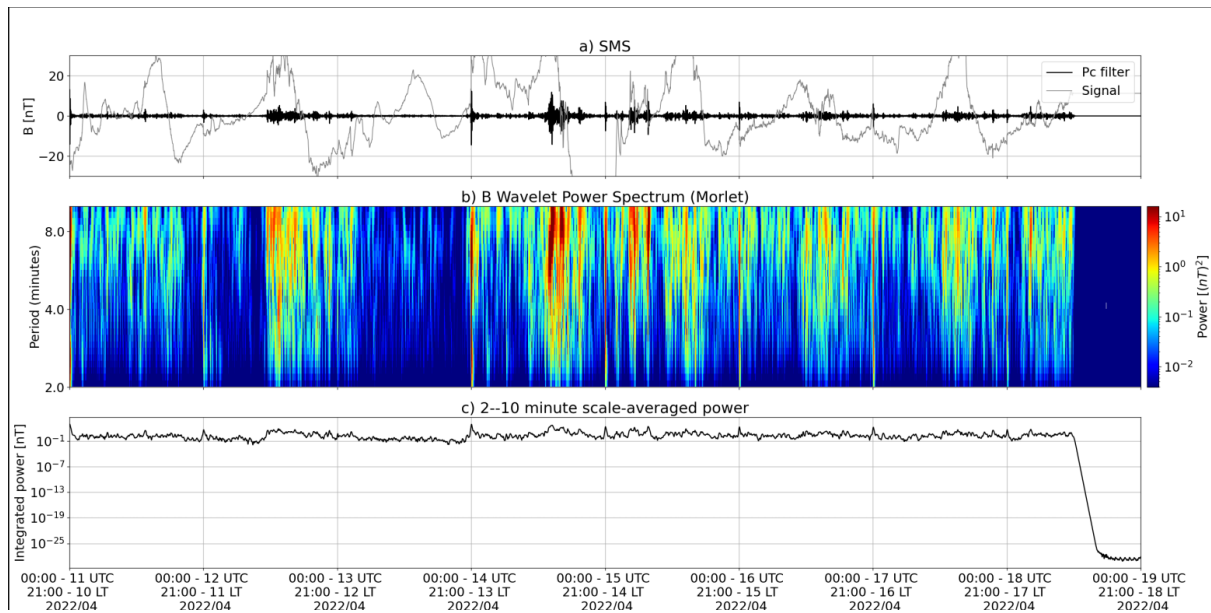
from the ARASE satellite are not available for the week under analysis to confirm the L-shell level of this referred electron flux decrease.

ULF waves in the Magnetosphere

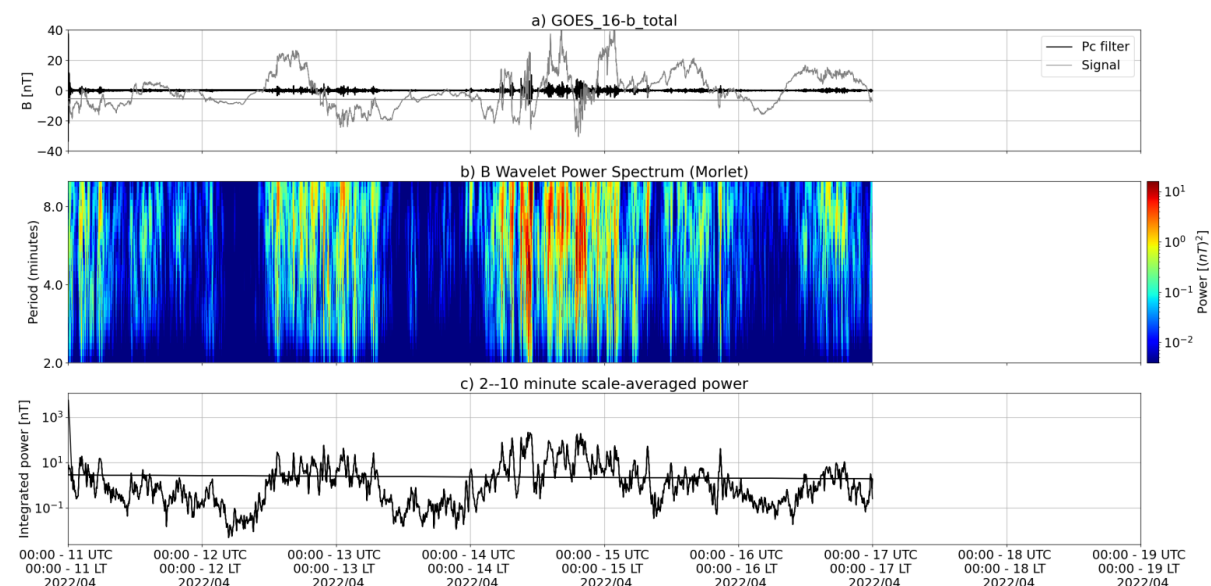
Responsible: José Paulo Marchezi



a) signal of the total magnetic field measured in the ISLL Station of the CARISMA network in gray, together with the fluctuation in the range of Pc5 in black. b) Wavelet power spectrum of the filtered signal. c) Average spectral power in the ranges from 2 to 10 minutes (ULF waves).



a) signal of the total magnetic field measured in the SMS Station of the EMBRACE network in gray, together with the fluctuation in the range of Pc5 in black. b) Wavelet power spectrum of the filtered signal. c) Average spectral power in the ranges from 2 to 10 minutes (ULF waves).

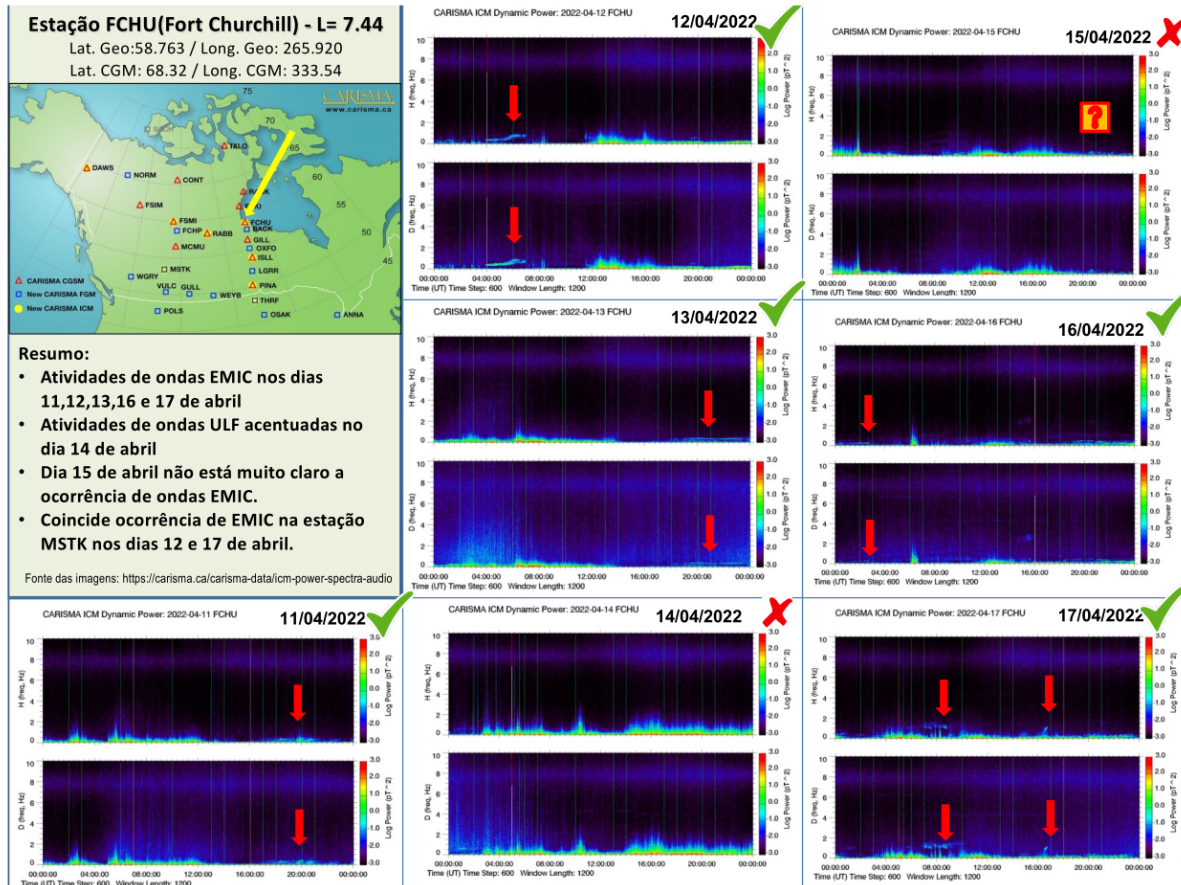


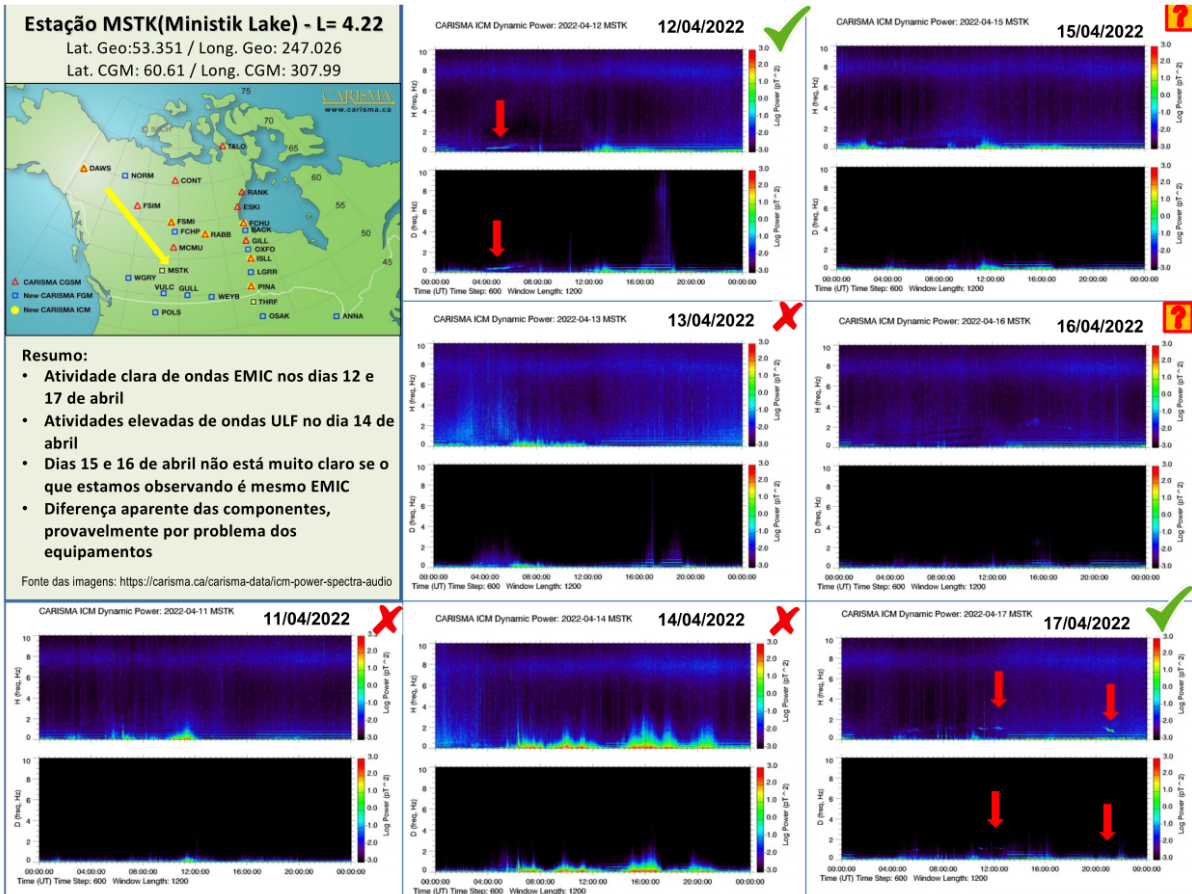
a) signal of the total magnetic field measured by the GOES 16 satellite, together with the fluctuation in the range of Pc5 in black. b) Wavelet power spectrum of the filtered signal. c) Average spectral power in the ranges from 2 to 10 minutes (ULF waves).

The ULF wave activity shows an increase in power from the 13th of April in the form of continuous pulsations, detected from high latitudes to the magnetometers at low latitudes of the EMBRACE network (Figure 2, SMS). On the 14th and 15th of April, new increases in ULF power are observed at high latitudes and with an impulsive characteristic on the 14th, with a permanence of fluctuations during the rest of the period, possibly associated with the interaction of a CME followed by an HSS.

EMIC waves in the Magnetosphere

Responsible: Claudia Medeiros



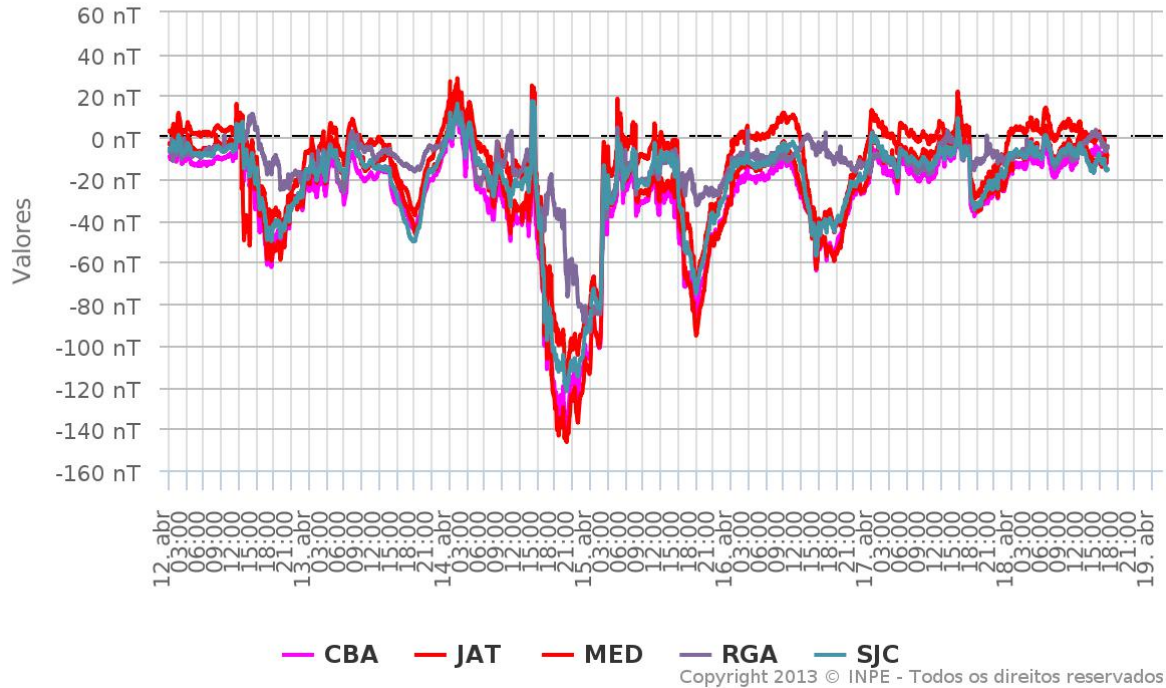


Geomagnetism

Responsible: Livia Ribeiro Alves

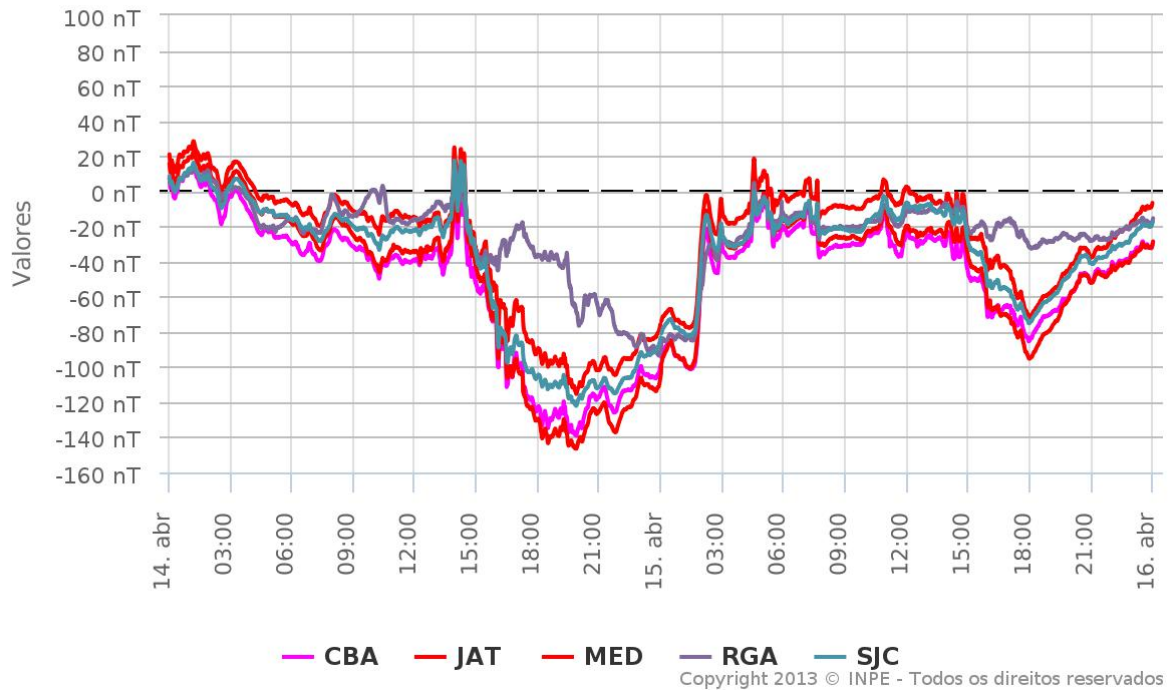
Rede EMBRACE de Magnetômetros

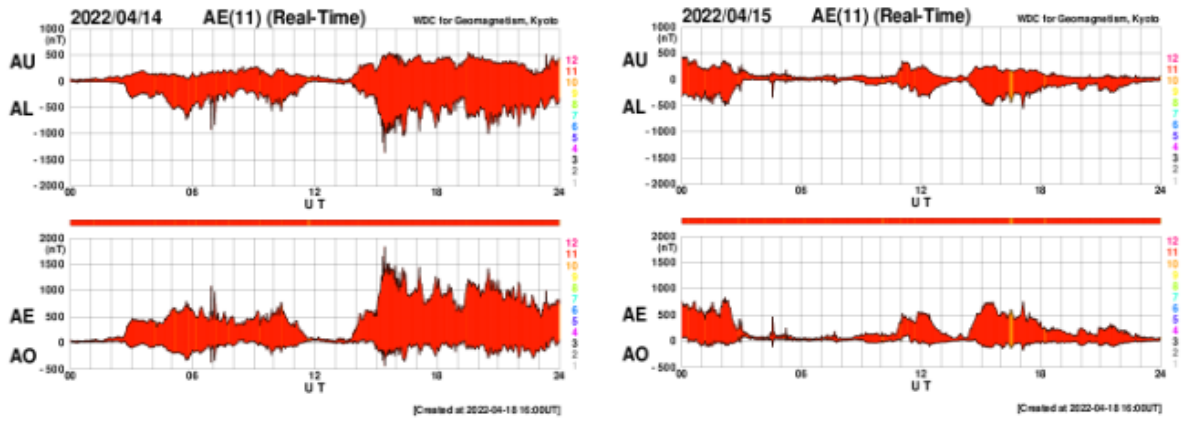
ΔH - (12/04/2022 - 18/04/2022)



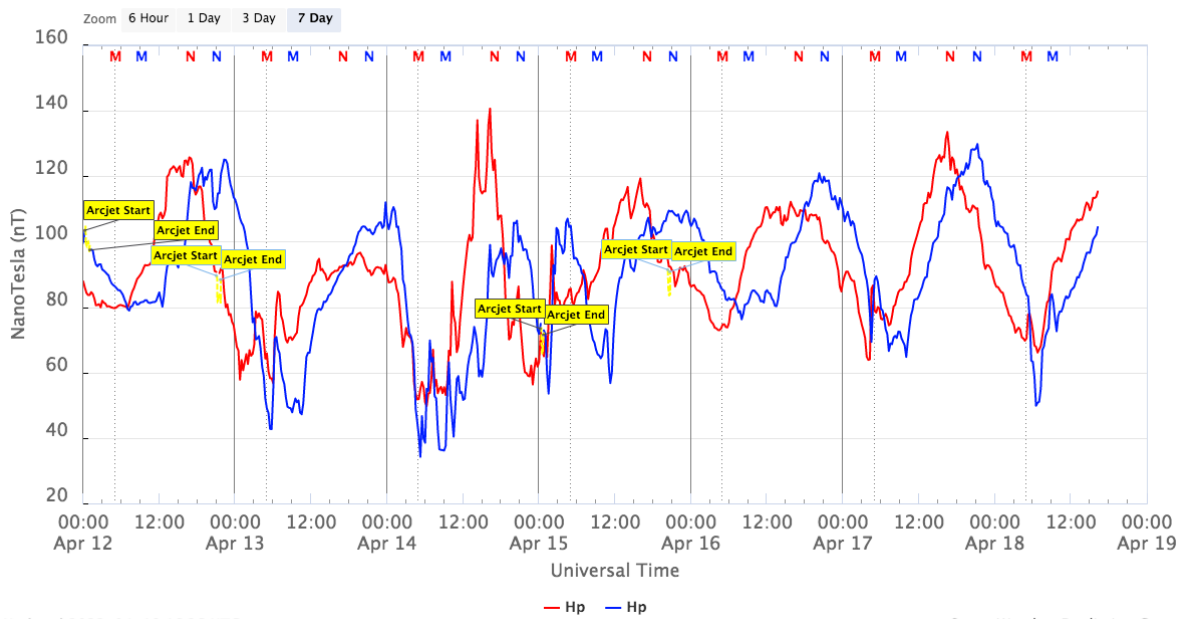
Rede EMBRACE de Magnetômetros

ΔH - (14/04/2022 - 15/04/2022)



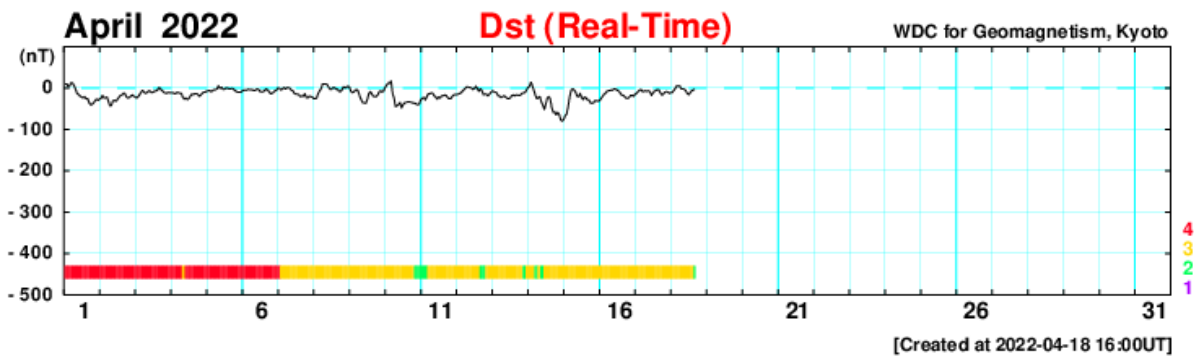


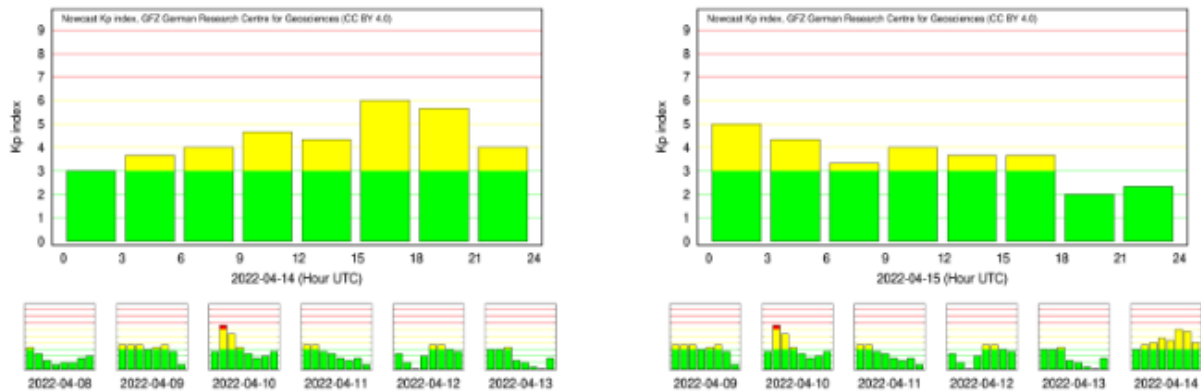
GOES Magnetometers (1-minute data)



Updated 2022-04-18 16:26 UTC

Space Weather Prediction Center





- The data from the Embrace magnetometer network showed instabilities throughout the period, maintaining the characteristic behavior of fluctuations and active periods. Featured events:
- April 14 and 15 - a drop of up to -140nT in the H component of the magnetometers
- The Dst index reached its minimum value of -80 nT on 14/10. The Highest Kp of the week was 60 recorded on April 14
- The auroral activity was intensified on April 14 and 15.
- Magnetic field measured in the orbit of the GOES satellite showed disturbances on April 12 and 14.

Ionosphere

Responsible: Laysa Resende

Boa Vista:

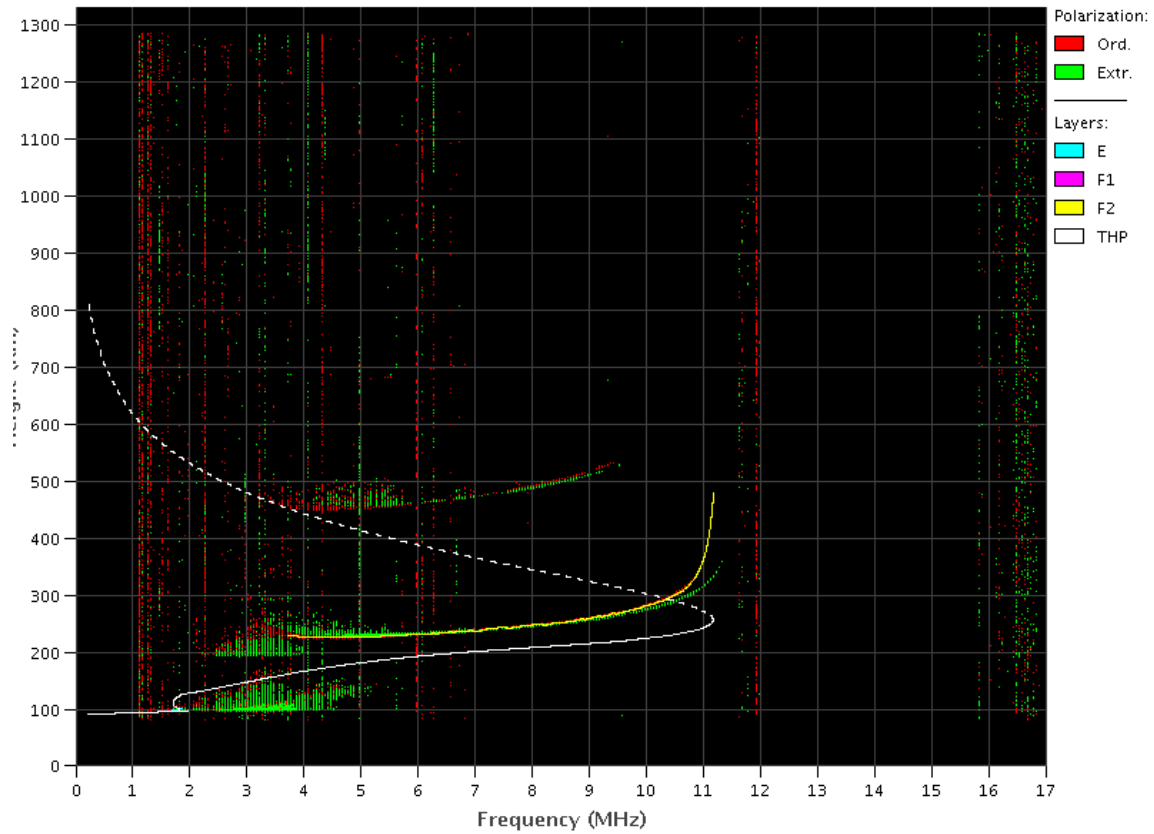
No Data.

Cachoeira Paulista:

- Do not occur spread F during the week.
- The Es layers reached scale 3 on days 12, 13, and 17.

EMBRACE – Digital Ionosonde

Cachoeira Paulista – 04/13/2022 20:20:00 UT

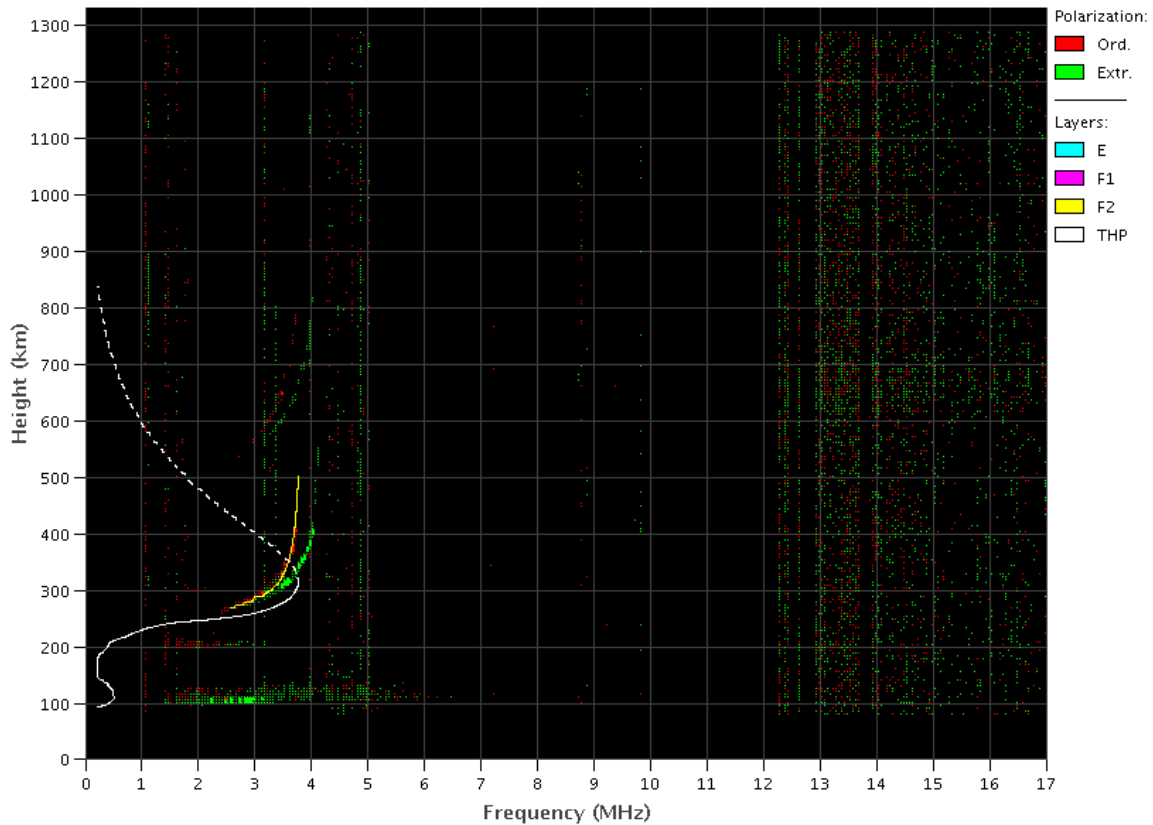


Fortaleza:

- There were spread F during all days in this week.
- The Es layers reached scale 3, and 4 during all days in this week.

EMBRACE – Digital Ionosonde

Fortaleza – 04/11/2022 07:00:00 UT

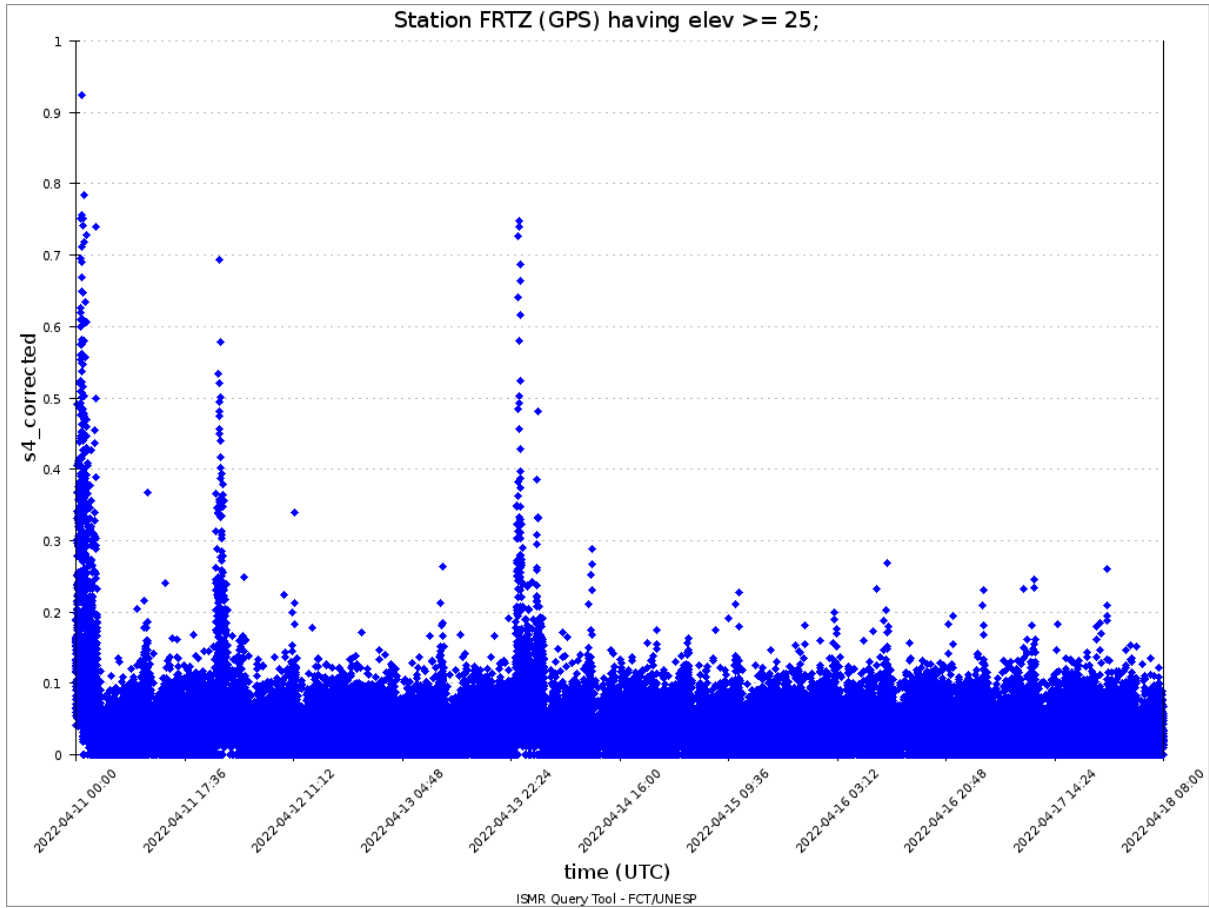


Scintillation S4

Responsible: Siomel Savio Odriozola

In this report on the S4 scintillation index, data from FRTZ in Fortaleza/CE, STSN in Sinop/MT, UFBA, in Bahía/BA e SJCE in São José dos Campos/SP are presented. The S4 index tracks the presence of irregularities in the ionosphere having a spatial scale ~ 360 m.

Moderate values of the S4 index (~ 0.5 — 0.7) were measured after the on 11, 12 and 13 /04 only for FRTZ and STSN stations (Figure 1). The UFBA and SJCE stations did not have any scintillation events, responding to the end of the bubble season in Brazil.



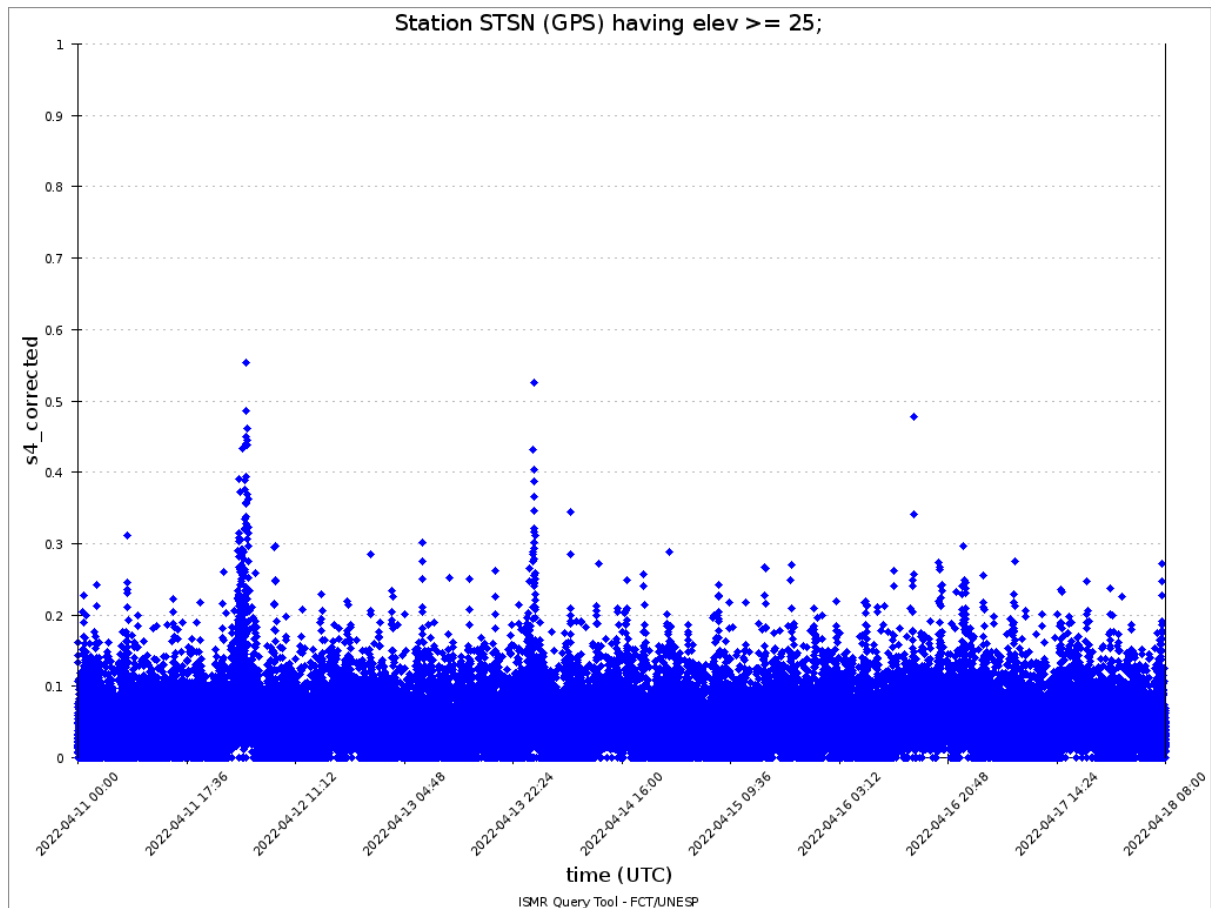


Figure 1: S4 index values for the GPS constellation measured at FRTZ (upper panel) and STSN(lower panel) during the week 04/ 11-18.

All-Sky Imager

Responsible: Cosme Alexandre

All-Sky Imager EPBs Observation || Apr 10 - Apr 16, 2022
Observações das EPBs por meio do imageador All-Sky -
|| 10 apr - 16 abril, 2022

Observatory Observatório	Apr 10 Abril 10	Apr 11 Abril 11	Apr 12 Abril 12	Apr 13 Abril 13	Apr 14 Abril 14	Apr 15 abril 15	Apr 16 abril 16
CA	✓☾	✓●	✓●	✓○	✓○	✓☾	✗
BJL	✓○	✓●	✓●	✓●	✓●	✗	✗
CP	✓●	✓●	✓☾	✓●	✓●	✗	✗
SMS	✓●	✓☾	✓☾	✓☾	✗	✓☾	✗
CA	São João do Cariri						
BJL	Bom Jesus da Lapa						
CP	Cachoeira Paulista						
SMS	São Martinho da Serra						
✓	Observation - Observação						
✗	No Observation - Sem Observação						
○	Clear sky - Céu limpo						
☾	Partly Cloudy - Parcialmente Nublado						
●	Cloudy - Nublado						
☼	Blur image - Desfocar Imagem						

- At the São João do Cariri observatory, plasma bubbles were observed only on April 10th. On the 11th and 12th the sky was cloudy. On the other hand, on the 13th and 14th the sky was clear. Finally, the 15th and 16th had few or no observations due to the full moon.
- At the Bom de Jesus da Lapa observatory between the 10th of April and the 6th of April, the sky was cloudy (days between the 11th and 14th) and without observation on the 15th and 16th. plasma only during day 10.
- At the Cachoeira Paulista no plasma bubbles were observed during the period. On the 10th, 11th, 13th and 14th of April the sky was cloudy. While the 12th was partially cloudy. Finally, April 15th and 16th were unobservable due to the full moon.
- Finally, at the observatory of São Martinho da Serra, a structure similar to the bright plasma bubble was observed on April 11th. On the other days, the OI 630 nm airglow was not observed due to nebulosity, moon and period without observation.

TEC

- Plasma bubbles were observed throughout the period. However, as the bubble seasonality is at the end, thus the plasma bubbles have small spatial dimensions and are difficult to observe on TEC maps.

ROTI

Responsible: Carolina de Sousa do Carmo

Week	Day	Time of occurrence (UT)
Sunday	2022/04/10	00:00-04:00; 07:30-11:00
Monday	2022/04/10	00:00-04:00; 22:30-24:00
Tuesday	2022/04/10	01:30-05:00
Wednesday	2022/04/10	22:00-24:00
Thursday	2022/04/10	00:00-04:30
Friday	2022/04/10	-
Saturday	2022/04/10	-

Table 1 – Weekly Summary (April 10-16, 2022).

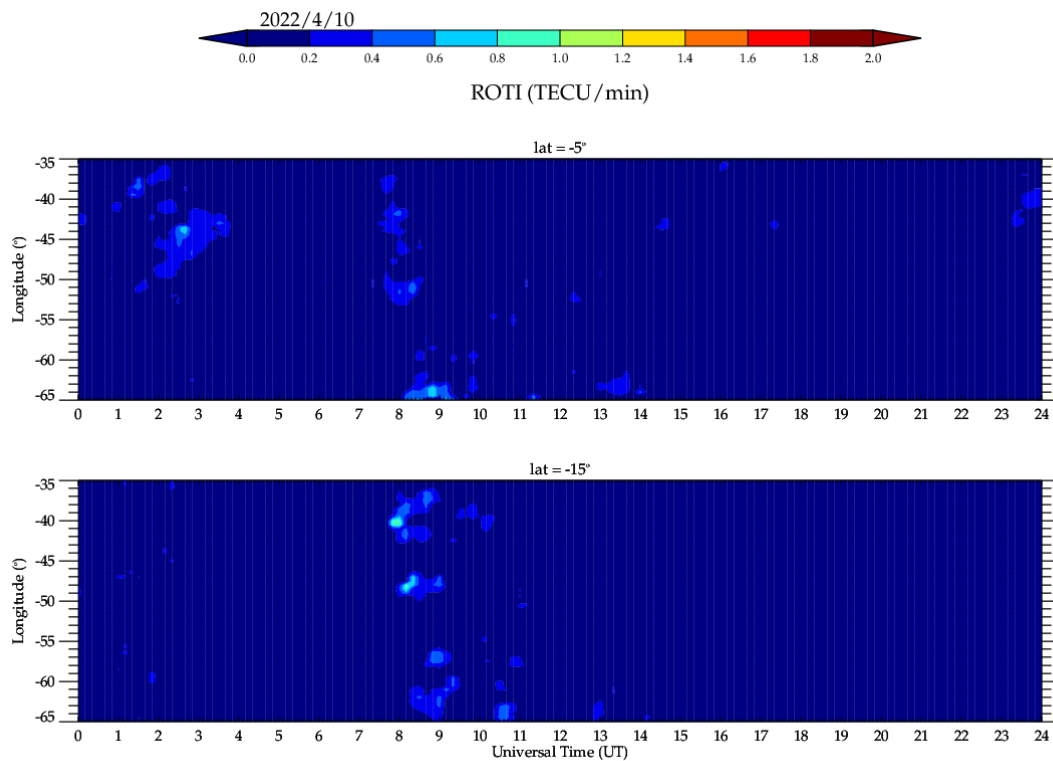


Figura 1 – Keograma do índice ROTI, para as latitudes geográficas fixas 5°S e 15°S, do dia 10 de abril de 2022.

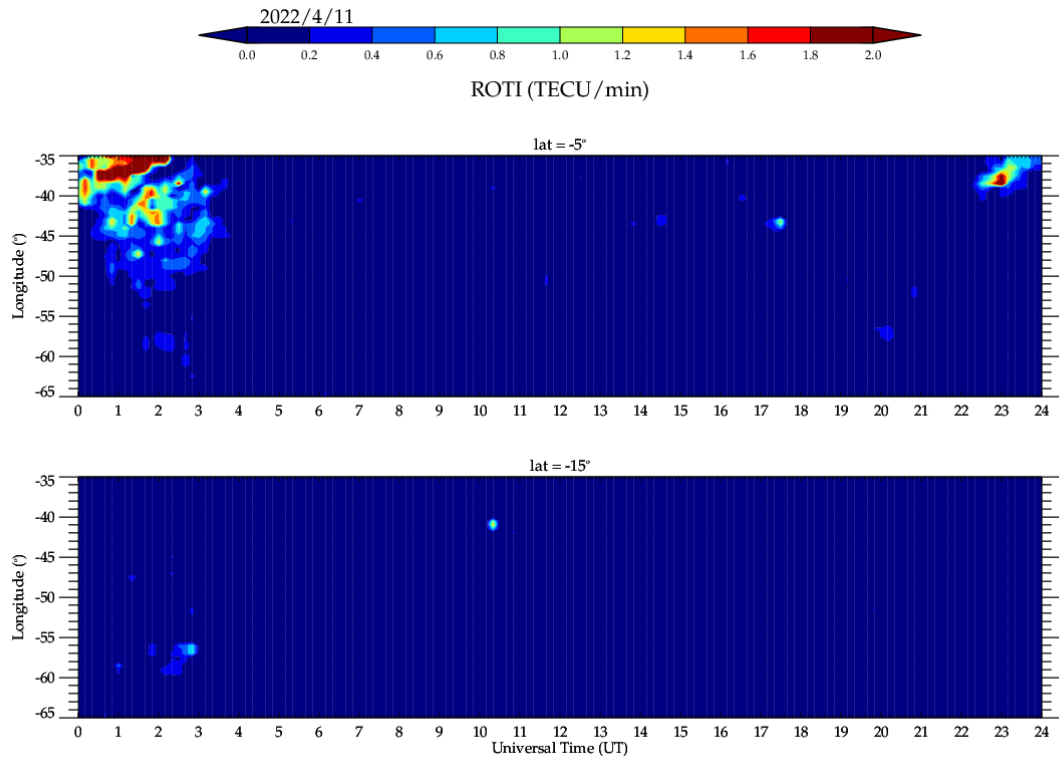


Figura 2 – Keograma do índice ROTI, para as latitudes geográficas fixas 5°S e 15°S, do dia 11 de abril de 2022.

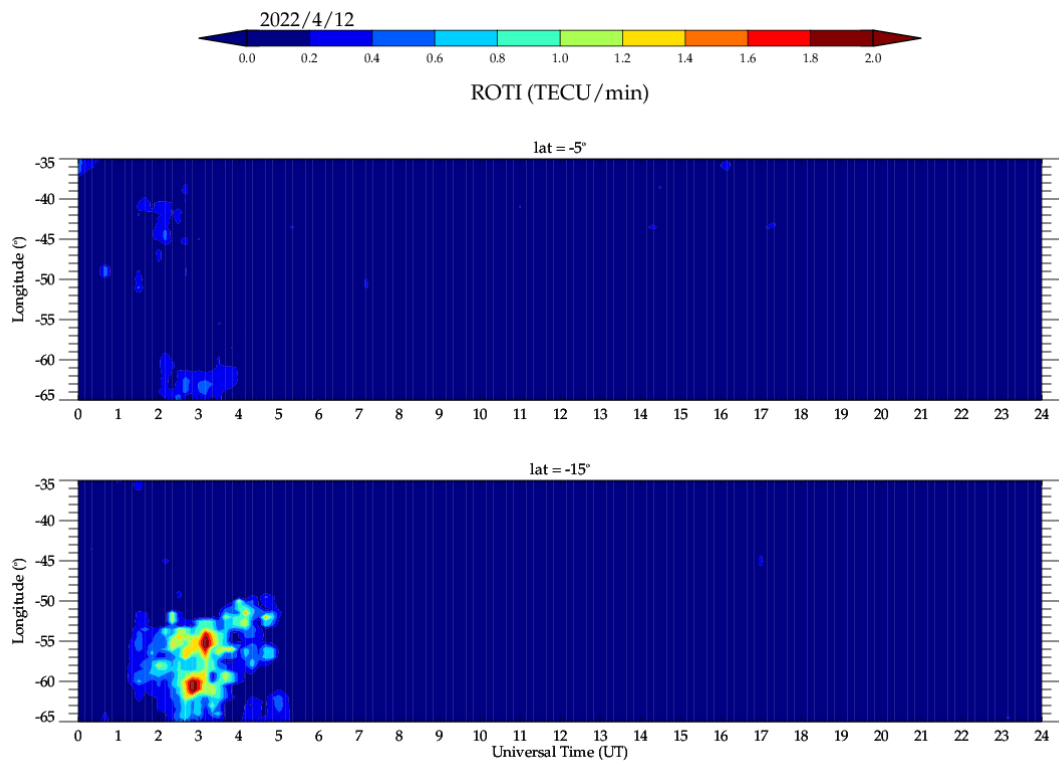


Figura 3 – Keograma do índice ROTI, para as latitudes geográficas fixas 5°S e 15°S, do dia 12 de abril de 2022.

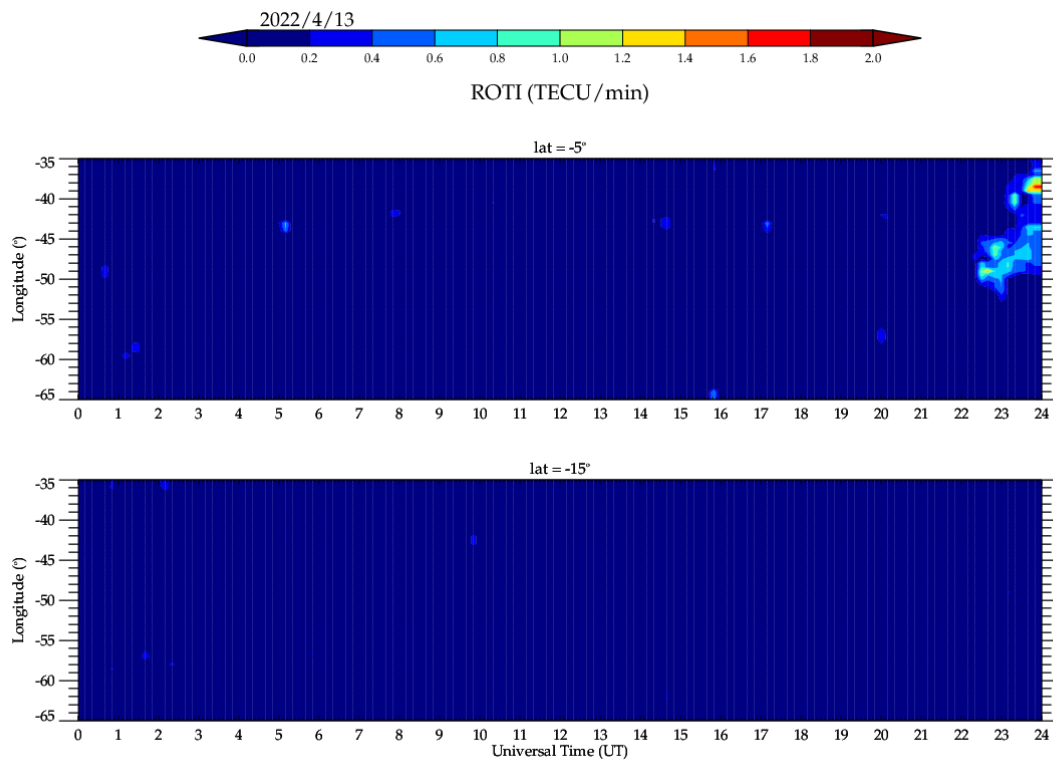


Figura 4 – Keograma do índice ROTI, para as latitudes geográficas fixas 5°S e 15°S, do dia 13 de abril de 2022.

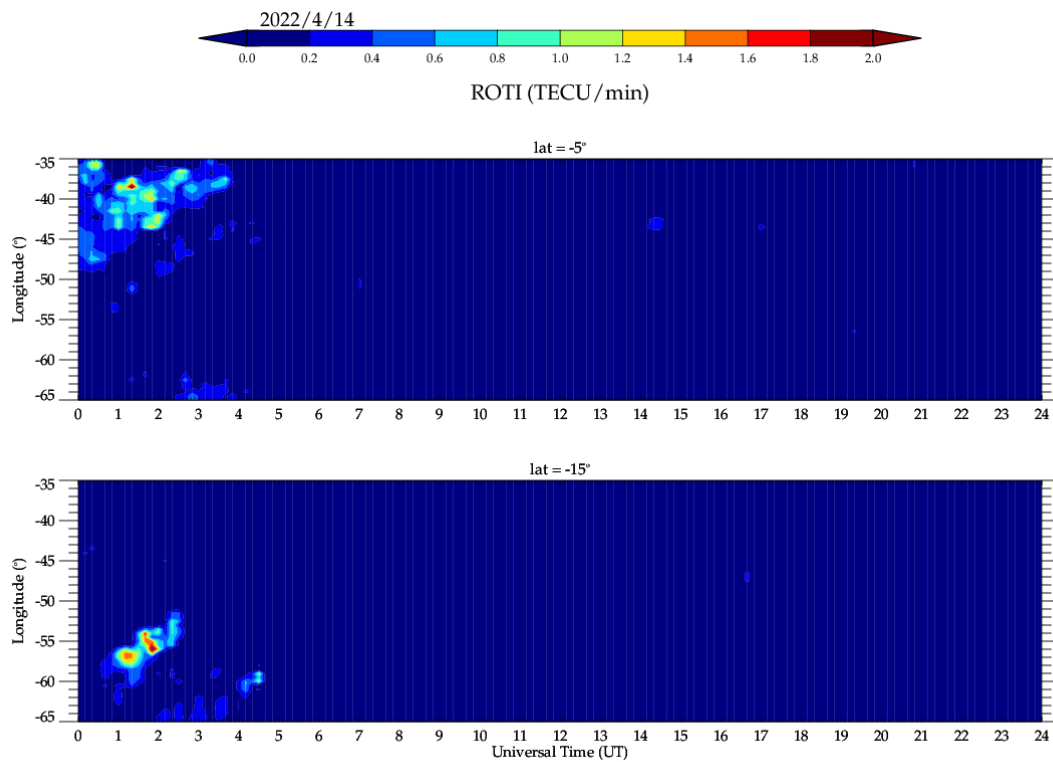


Figura 5 – Keograma do índice ROTI, para as latitudes geográficas fixas 5°S e 15°S, do dia 14 de abril de 2022.

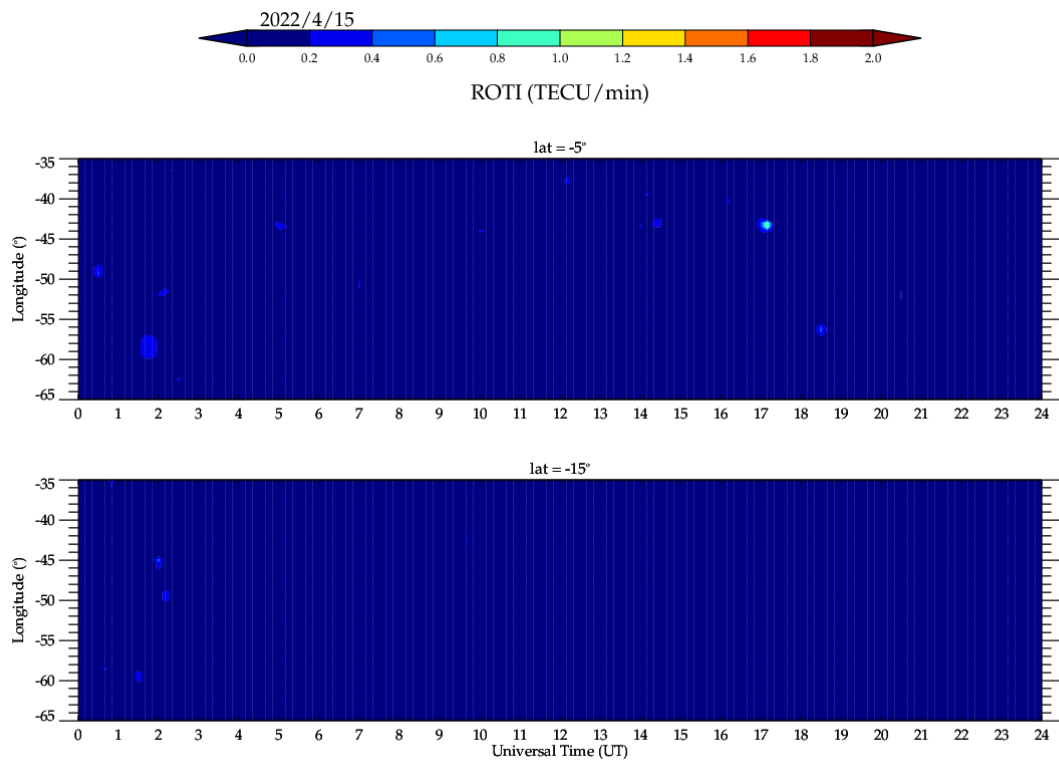


Figura 6 – Keograma do índice ROTI, para as latitudes geográficas fixas 5°S e 15°S, do dia 15 de abril de 2022.

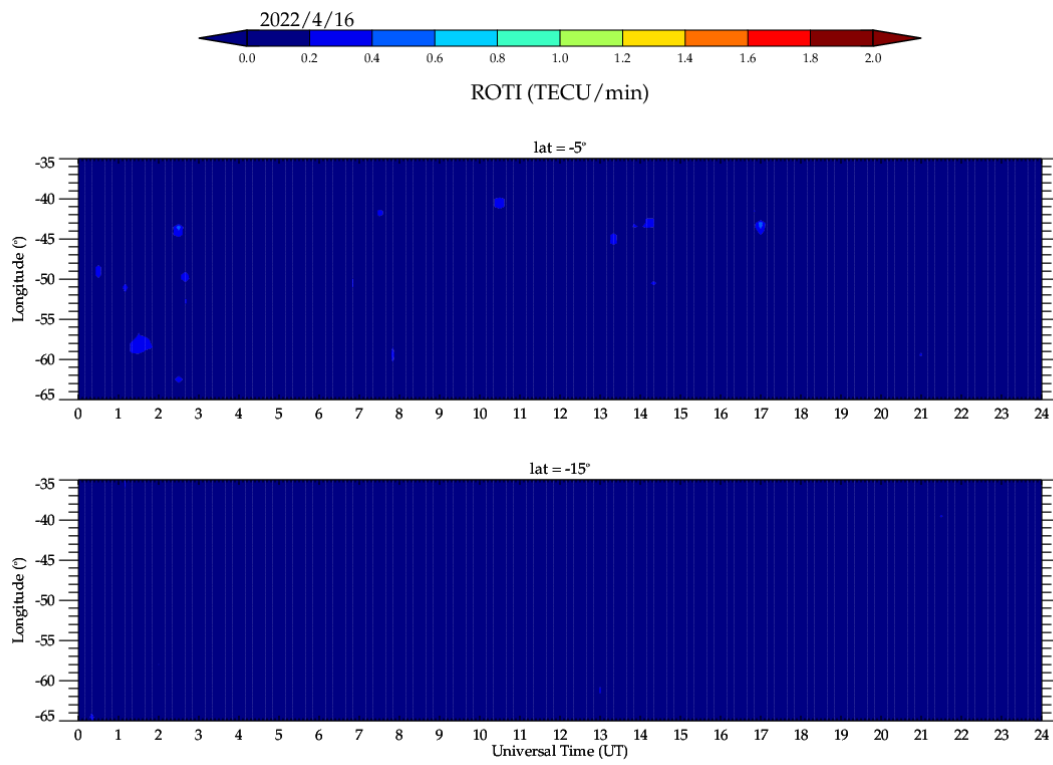


Figura 7 – Keograma do índice ROTI, para as latitudes geográficas fixas 5°S e 15°S, do dia 16 de abril de 2022.